Journal of Mineralogical and Petrological Sciences, Volume 97, page 153-160, 2002 Sueno Issue

A Raman spectroscopic study of shocked forsterite

Isamu SHINNO

Graduate School of Social and Cultural Studies, Kyushu University, Ropponmatsu 4-2-1, Chuoku, Fukuoka, 810-8560, Japan

The profiles of Raman spectra below 670 cm^{-1} of synthetic single crystals of forsterite shocked up to 82 GPa were analyzed. Up to the shock pressure of 46.2 GPa, Raman bands of Si-O external vibrations of translational and rotational modes are linearly shifted without band broadening to higher frequencies with the increase of the residual strain caused by shock pressure. The Mg(M2)-O translational band is not shifted, but broadens linearly with the strain increase. Normalized band shift and broadening are used to compare the variation. These variations show that differential residual stress and strain still remain within cation polyhedra. The dependence of the normalized broadening on the pressures less than 46.2 GPa is formulated, and this relation can be used to estimate the shock pressure of chondritic olivne. Many extra Raman bands are found in this region, implying that the forsterite may be partly transformed into unknown phases.

Introduction

Under a static pressure at relevant temperatures, it is well-known that forsterite exhibits three polymorphs of phase transformation. At ambient temperature, it was confirmed by X-ray diffraction and Raman spectroscopy, that a second-order phase transition occurred at 8 or 9 GPa (Kudoh and Takeuchi, 1985; Chopelas, 1990; Wang et al., 1993). Under shocked compression states, three critical points were detected on a Hugoniot diagram for forsterite, i.e., the Hugoniot elastic limit (HEL) at 10 GPa, the onset pressure of phase transition at 50 GPa and the decomposition pressure of forsterite at 96 GPa (Syono et al., 1981). Various transition pressures of forsterite are summarized in Table 1.

Miyamoto and Ohsumi (1995) have successfully detected a Raman shift and broadening in the internal Si-O stretching vibration band near 820 cm^{-1} of olivine in L6 ordinary chondrites. They confirmed the residual stress caused by a strong impact shock in olivine was still remained. Recently, extensive works to detect residual lattice strain have been done in artificially shocked forsterites (Uchizono et al., 1999; Shinno et al., 1999; 2000a; 2000b), where the strain was estimated from their X-ray diffraction peak-broadening by using a Williamson-Hall plot (Wilson, 1962). It was found that the shocked forsterite gave rise to eight broad bands in photo-luminescence spectra in contrast to the normal forsterite, usually exhibiting only faint and obscure luminescence. Since such luminescent centers were usually formed near dislocations due to internal friction or elastic stress in a crystal. This type of luminescence in the shocked forsterite was called "deformation-sensitive luminescence" (Shinno et al., 2000b).

The studies on deformation-sensitive luminescence showed clearly a close relationship between the photo-luminescence variation and the Raman band shift and broadening caused by variable degree of the residual strain in the crystal. The strain detected by the X-ray diffraction peak increased linearly with the shock pressure up to 82 GPa, while broadening and shift of the Raman band and the intensity of the luminescence band were sensitively changed at 46.2 GPa. The critical shock pressure of 46.2 GPa is very close to the onset shock pressure of the phase transition at 50 GPa on the Hugoniot curve of forsterite (Syono et al., 1981). This phase transition may indicate a higher-order phase transition of the shocked forsterite.

The variation of the broadening of the X-ray diffraction peak and the intensity of photo-luminescence with that of the shock pressure were successfully formulated and applied to estimate the shock pressure of Dhurmsala LL6 chondrites (Uchizono et al., 1999; Shinno et al., 1999).

Usually, the modes associated with the internal stretching and bending within the SiO_4 tetrahedron above 450 cm^{-1} have weak pressure dependence to those associated with the external lattice vibrations such as the translational and rotational Mg(M2)-O and Si-O vibrations below 450 cm^{-1} (cf. note in Table 1). In this report, extra Raman bands and normalized broadening and shifting of some Raman bands below 670 cm^{-1} in the shocked forsterite were examined. Other features of Raman band characteristics were already presented in a

I. Shinno, Shinno@rc.kyushu-u.ac.jp Corresponding author

Table 1. Reported transition pressures for forsterite

	Critical pressure (GPa)			Phenomena		Remarks & references
Static	12.9		(at 1000°C)	α—β transition		Morishima et al. (1994)
	17.2		(at 1000°C)	β—γ		Suzuki et al. (2000)
	21.1		(at 1600°C)	decompose γ to MgO + $MgSiO_3$		Irifune et al. (1998)
	8.0		(at a.t.)	M1-O bond, cease shortening		Kudoh and Takeuchi (1985)
	~15~		(at a.t.)	Si-O, M2-O bond continue to short		ibid.
	16		(at a.t.)	Complete to form oxygen hcp lattice		ibid.
			(below a.t.)	Raman band (cm^{-1})		† Wang et al. (1993)
	7.0†*	*(7.0)*†*	(8.9)‡*	306	M2-O t	‡ Chopelas (1990)
	8.0	*(11)*	(9.2)	545	Si-Ov4	
	8.5	*(9.0)*	(9.2)	227	Si-O t	t : translational mode
	9.0	*(7.5)*	(9 .1)	856	Si-Ov1+v3	v: stretching
	10.9	*(8.0)*	(9.0)	341	Si-O r	r : rotational
			(9.2)	585	Si-Ov4	
Shocked	10		(at s.e.)	Hugoniot elastic limit		Syono et al. (1981)
	50			Phase transition, Abrupt change of deformation luminescence		Syono et al. (1981); Shinno et al. (1999)
	96			Decomposition of forsterite		Syono et al. (1981)

a.t., ambient temperature; s.e., shocked event, temperature raised, but its precise value is not known.

* These values are the change of slope of pressure dependence for Raman bands with individual mode shown in the right column, which show the change of compression mechanism of forsterite under high pressures. The values in Italic are under quasi hydrostatic. Some data of pressure dependence of Raman band shift (cm^{-1}/ GPa): M2-O t 3.26-3.9, Si-O t 1.1-1.2, Si-O r 4.7-5.0, Si-O v 1.8-2.3 (Chopelas, 1990).

previous report (Shinno et al., 2000a).

Experimental

As the shock experiment and the treatment of recovered sample of synthetic forsterite have already been described by Uchizono et al. (1999), a brief explanation is given below:

Sample preparation

The recovered forsterites was polished to a thin section, where each sample was cut approximately along the shock compacting direction parallel to the crystallographic ***a***-axis of forsterite. However, appropriate crystallographically oriented samples to measure a polarizing Raman spectrum could not be prepared due to metal sample container with dynamic compression of forsterite hardened and enveloped too strongly to separate crystal.

Microscope Raman spectroscopy

Raman spectra were measured by a polarized laser Raman microscope-spectrometer (Ramanor –T–64000) at room temperature. The main experimental conditions were as follows: The Ar 488.0 nm beam with a range of 100-200 mW was used. An objective lens 90x with N.A. 0.75 was very effective for collecting a weak signal. The polarized laser light was focused to form a beam spot of 1 μm in diameter on the sample placed at the diagonal position of the forsterite on the polarized microscope stage. Unpolarized Raman signal was collected from a back-scattering geometry and entered to the triple monochromator. A charge-coupled device (CCD) system cooled with liquid nitrogen was used for recording the spectra. The CCD system was a useful tool for detecting weak signals efficiently for a wide multichannel range of 200 to 670 cm^{-1} at the subtractive mode. A detailed description was given in the previous report (Shinno et al., 2000a).

Profile analysis

The observed spectrum of shocked forsterite has usually a large background composed of photo-luminescence due to lattice deformation. Therefore, Raman spectrum appears with baseline increasing for high frequency region (Fig. 1a). Although Heymann and Cellucci (1988) and Heymann (1990) have reported many Raman spectra of shocked olivines, they have failed in analyzing their spectra of the region because of poor spectra hidden behind the strong background. In this study, the background was fitted to a profile with a

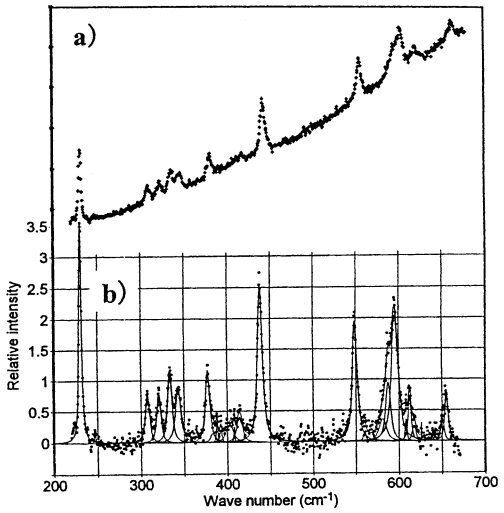

Figure 1. Raman spectra of forsterite shocked at 46.2 GPa. a) Raw Raman spectra with large background, i.e. deformation-sensitive luminescence, b) Calculated spectra with deconvoluted peaks by the fitting to Voigt functions are displayed as solid lines (ref. Table 2) (the background was removed).

quadratic equation. Consequently, the profile analysis to obtain the precise component-band parameters in the spectra has been done by a Voigt function with no constraints after subtracting the background from the observed spectra.

Results and Discussion

Raman spectra in the range of 200-1000 cm^{-1} and their characteristics of the band shift and broadening for the present shocked forsterites have already reported by Shinno et al. (2000a). A typical example of observed Raman bands of shocked forsterite at 46.2 GPa is given in Figure 1a. Their parameters are summarized in Table 2. Band parameters of so called external lattice vibrations of translational, rotational and an internal asymmetric stretching mode are given in Table 3. In this table the residual strain derived from the previous report (Uchizono et al., 1999) are also given. Usually, the profile analysis permits to determine the band position precisely with an error less than 0.1 cm^{-1}, which is smaller than a pixel value of 0.49 cm^{-1} in the CCD detector. On the other hand, the bandwidth contains a large error depending on the band intensity, so the tendency of variation according to the shock pressure cannot be directly read from the table.

The shape parameter for the Si-O translational band shown in Table 3, a mixing ratio of Lorentzian and Gaussian functions in a Voigt function, does not show any correlation with the shock pressure. The least squares fitting is successful for obtaining the band parameters with relatively low statistical error when using the Voigt function. Hereafter, the author will discuss only the results in relation to normalized Raman band shift and width to reduce the statistical and the apparatus response error, and the chemical mass effects on the parameters may be eliminated through this procedure.

Table 2. Examples of Raman band parameters obtained by profile analysis*

Peak No.	Mode	Intensity	Position (cm^{-1})	Width
1	Ag	3.60(5)	230.8(1)	1.02
2	B2g	0.173	246.8	0.341
3	Ag	0.677(36)	307.5(15)	3.23(53)
4	B1g,3g	0.666	320.6	2.36
5	Ag	1.03(5)	333.5(1)	2.72(49)
6	Ag	0.786	343.0	2.97
7	B3g	1.05(3)	377.6(1)	2.23(31)
8	?	0.306	387.8	0.605
9	?	0.280	392.1	0.482
10	?	0.233	399.0	0.355
11	?	0.356	403.6	0.335
12	?	0.301	407.9	0.471
13	B3g	0.395	414.2	1.18
14	B2g	2.44(3)	438.4(1)	2.30(24)
15	Ag	1.92(4)	548.6(1)	1.56(35)
16	?	0.178	560.2	1.24
17	B1g	0.325	581.9	1.01
18	B2g	1.21	588.4	2.24
19	B3g	1.82	595.8	2.93
20	?	0.255	602.5	1.07
21	Ag,?	0.373	607.7	0.738
22	Ag	0.716	612.2	1.12
23	B1g,?	0.269	617.4	1.05
24	?	0.146	625.8	0.693
25	B1g	0.142	635.2	0.387
26	?	0.163	641.2	1.10
27	?	0.449	650.4	0.916
28	?	0.691(39)	654.4(2)	0.437(50)
29	?	0.321	657.2	0.565

* Sample: Forsterite shocked at 46.2 GPa (Fig. 1). Standard deviations are given in parentheses. The relative errors for data without standard deviations are larger than 20 %.
"?" in the mode column: extra bands.

Raman extra bands

The weak overlapping features on Raman spectra are always observed in the frequency range 200-650 cm^{-1} for shocked forsterites (Fig.1a), and detected extra bands are summarized in "synthetic" column of Table 4, where Raman band data for non-shocked volcanic and shocked chondritic olivines are given for comparison. The typical extra band near 650 cm^{-1} position is composed of 1 to 3 bands and has a tendency to become clear and intense with the increasing shock pressure. Thus this is a noticeable band considered as an extra broad band.

The presence of extra bands could be due to the

Table 3. Mean values of Raman band parameters for main bands

Sample	F0	F10	F20	F35	F46	F53	F60	F82
Shock *P* (GPa)	0	11.7	20.8	34.5	46.2	52.8	61.2	82.0
Residual S	0.034	0.071	0.099	0.15	0.19	0.22	0.25	0.30
s-t p (cm^{-1})	229.9	230.5	230.4	230.8	230.9	231.1	231.1	230.9
w (cm^{-1})	2.28	1.41	1.90	2.14	1.85	1.76	1.80	1.61
s	0.06	0.48	0.03	0	0.22	0.36	0.84	0.36
m-t p (cm^{-1})	307.4	307.9	307.4	306.8	307.8	307.4	307.8	307.3
w (cm^{-1})	1.85	2.16	2.62	2.70	3.29	3.88	3.89	4.11
s-r p (cm^{-1})	331.7	332.0	332.5	332.6	334.1	333.6	334.3	333.9
w (cm^{-1})	1.95	2.12	2.58	3.48	3.42	2.55	2.87	3.36
s-s p (cm^{-1})	545.0	545.5	545.6	545.8	546.0	546.1	546.1	546.3
w (cm^{-1})	4.20	3.27	3.56	2.87	3.53	3.37	4.05	4.05

Abbreviations in the most left column: Shock *P*, shocked pressure; Residual S, residual strain obtained by a Williamson-Hall plot (quoted from Uchizono et al., 1999); Raman band assignment: s-t, SiO_4 translational mode ; s-r, rotational mode ; m-t, M2 translational mode; Band parameters: p, position ; w, bandwidth ; s, shape (mixing ratio of Lorentzian and Gaussian functions in a Voigt function, s =0 shows pure Lorentzian).

presence of other phases such as wadsleyite, ringwoodite, stishovite, coesite, MgO and Mg-perovskite. However, no Raman bands from such phases were found and also this result was confirmed by the X-ray diffraction and electron microprobe analyses (Uchizono et al., 1999).

As to the band assignment and some extra bands, there were some disagreements in previous study, especially in the lower to middle energy region. There are many bands in individual modes assigned by Chopelas (1991), which are not assigned by Price et al. (1987). These bands are indicated by @ in Table 4. The contractive cases are indicated by "t" in Table 4. Extra bands such as 402, 650 nm^{-1} bands, which are almost always found in forsterite Raman spectra with relatively high intensity, have not been assigned yet. Therefore, the assignment for Raman band is examined referring to the studies of Paques-Ledent et al. (1973), Servoin and Piriou (1973), Price et al. (1987) and Chopelas (1991). These data for non-shocked synthetic forsterite and natural olivine and shock-experienced meteorite olivine are summarized as shown in Table 4. Many extra bands were detected but the intensity of the shock was not analyzed in this stage of study. There are reports dealing with the extra bands appeared in the forsterite structure under hydrostatic pressures (Reynard et al., 1994; 1996). Extra bands appearing in volcanic and chondritic olivines were also reported (Table 4, Ooba and Shinno, 1996). Some extra bands for forsterite under various hydrostatic pressures can be seen in the spectra reported by Chopelas (1990).

Reynard et al. (1994) have studied Mg_2GeO_4 as a good analogue of forsterite with increasing quasi- and non-hydrostatic pressures, and they found extra bands in the range 600-700 cm^{-1}. They interpreted these bands correspond to those from the progressive metastable transformation phase, which was thought to be a high-pressure phase close to the spinelloid formed from olivine. They also referred to the phase appearing in the mixed-phase region of the high shock pressure in Hugoniot of olivine, whose phase was a random close-packed phase coexisting with olivine at the shock pressure between 40 and 80 GPa (Jeanloz, 1980 a; 1980 b). Although this phase has not been confirmed yet, it may be a structurally disordered spinelloid close to ω- or ε*-phase formed by shearing along every other (100) forsterite plane (Hyde et al., 1982; Madon and Poirier, 1983; Reynard et al., 1994). A spinelloid has polymerized Si_2O_7 units as seen in the melilite group, in which strong vibrational bands of Si-O-Si appear in the range 626-664 cm^{-1} (Shinno, unpublished data).
Based on the above considerations, some extra bands at around 400 and 650 cm^{-1} may be caused by the phase close to the disordered spinelloid having a polymerized bond of Si-O. Although the stable wadsleyite, a spinelloid, has two strong peaks at 723 and 918 cm^{-1} for the polymerized bond (MacMillan and Akaogi, 1987) nearly corresponding to forsterite own bands, the other proper bands belong to these two minerals do not coincide to the present observed Raman bands. The strain by shock compression may cause the reduction of symmetries of forsterite structure, and produces some forbidden and combined vibrational modes. At this stage, however, I was unable to assign clearly these extra peaks.

McMillan et al. (1992) have detected also extra bands in single crystalline quartz shocked to above 22GPa, and show that thses bands were due to the formation of high density SiO_2 glass. In the present shocked forsterite, amorphization was not detected by a precise microscope Raman examination.

Normalized Raman band shift and broadening

As shown in Tables 2 and 3, the Raman band parameters

Table 4. Comparison of Raman bands (cm^{-1}) among non shocked synthetic forsteirte and natural olivine and shocked meteorite olivine

Asn	synthetic	Natural†	Chondrite‡	Asn	synthetic	Natural†	Chondrite‡
A_g				B_{1g}			
s-t	183	187sh	184		*164		
	t221	213sh	207		*197		
s-t	227s		238b		@220		
m-t	305s	296-310w		s-t	t231		(A_g)
	t312			s-t	@274		
s-r	328.5	327b		s-r	317s	316b	
m-t	339.5s				t325		
	t360	359b			t337		335s
ν2	424	425s		m-t	@351		383
ν4	545s	540s	547	m-t	@383s		419
	t580				418	425(A_g)	
ν4	609s	612b			t428	435-439sh	
	t630			ν2	434s		
	t807		812s		t454	584-586-592	
ν13	825.5s	824s	823-826s	ν4	583	612s	
ν13	856s	855-859sb	852		t617	634	641
	t943		937-944sb	ν4	632		660s
ν3	966s	955b	955		t667	667s	
B_{2g}	t149				t821		
mx	@175			ν1	839s	?	840s
	t207			ν3	866s	859	872
mx	244s		243-246		t963	971	
mx	324	327b		ν3	975.5		
	t345	349sh		B_{3g}	t133		133sh
mx	365	359-367s			t250		
	*407	412	408	mx	@286		287sh
	t433			mx	314		314w
ν2	438s		440-442		t327		
ν4	585s	586sh	583	mx	374s		
	t611				t390	379	395b
ν3	881s	882sh	872-882b	ν2	406		408b
	t901				t417	405-407	
Extra	402	122sh	496w, 671	mx	@435	417	
Bands	482	504s	678, 689b		*466	435	
	521	735sh	722, 725,		*484	468-462	
	650s	784sh	740, 772-774s	ν4	591s		
	739		999?,1007		t606	594sh	
	777		1014, 1038, 1086	ν3	920s	599-604	918s
					t960	919s	

Asn: Assignments were quoted from the following papers. A symbol attached on a wave number in the synthetic forsterite column is a unique band to the individual paper.

*, Servoin and Piriou (1973); @, Chopelas (1991); t, Price et al. (1987).

†, olivine in two-pyroxene andesite (Fo83). ‡, olivine in Yamato 790523 and 790757 meteorites (Ooba and Shinno, 1996).

In assignment column: ν1, SiO_4 internal mode symmetric stret ; ν2, internal mode ; ν3, internal mode asymmetric ; ν4, internal mode; mx, mode mixing band ; ν13: ν1+ν3, The symbol following the wave number; s, sharp and strong band ; w, weak, sh, a band on a shoulder, b, broad band. For other symbols, refer to Table 3.

obtained by the profile fitting method generally contain larger errors, especially with regard to the bandwidth. There are many mixed-mode bands with weak intensity, as the crystal is not oriented correctly to the polarized incident laser beam and a large background arising from photo-luminescence appears. Therefore, precise examination and explanation in this region are limited.

The band shift and width were strongly affected by the apparatus response during measurement of the spectrum and the mass effect of a sample (Shinno et al., 2000a). Even more, the band shift is very small within the shock pressure ranges. On the other hand the bandwidth broadens extensively with the substitution of other cations for Mg. Therefore, we need other appropriate parameters to characterize the shocked forsterite.

Normalized Raman band shifts of the shocked forsterite due to the shock pressure are shown in Figures 2 and 3. The wave numbers of rotational and traslational Si-O vibrations at around 333 and 230 cm^{-1} are divided by the wave number of the translational Mg(M2)-O band nearly unshifted from 307 cm^{-1}.

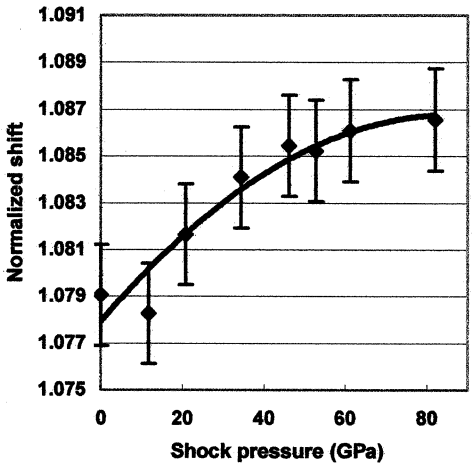

Figure 2. Normalized Raman band shift of Si-O rotational mode (333 cm^{-1}) vs Mg(M2)-O translational band (307 cm^{-1}).

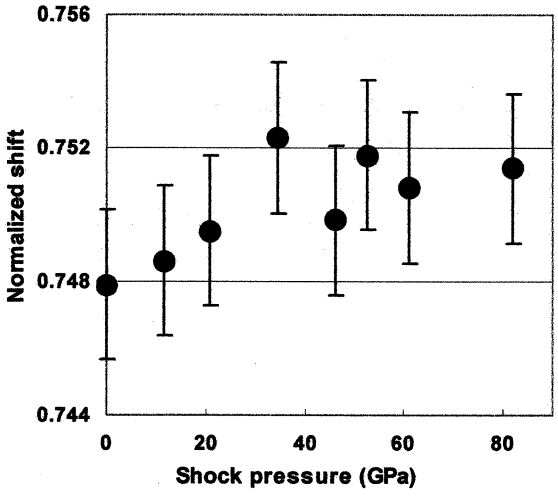

Figure 3. Normalized Raman band shift of Si-O translational mode (230 cm^{-1}) vs Mg(M2)-O translational band (307 cm^{-1}).

Since the Mg-O band shift is almost independent to the pressure, the variation between the shifts of the translational and rotational bands of the Si-O bond with the pressure can be clearly seen. The normalized rotational vibration of Si-O band varies uniformly with increasing pressure up to 82 GPa (Fig. 2), while the normalized translational vibration of the Si-O bond exhibits scattering with respect to the changes of Mg-O vibration and the pressure (Fig. 3). Above a shock pressure of 35 GPa, the normalized shift to higher frequencies of the translational mode is stopped, because the Mg-O band has a unique tendency to shift to lower frequencies above 46.2 GPa (Fig. 6 in Shinno et al., 2000a), even though this is not seen in Table 3. These features may show that the Mg-O translational vibration is cooperative to the Si-O rotational vibration,

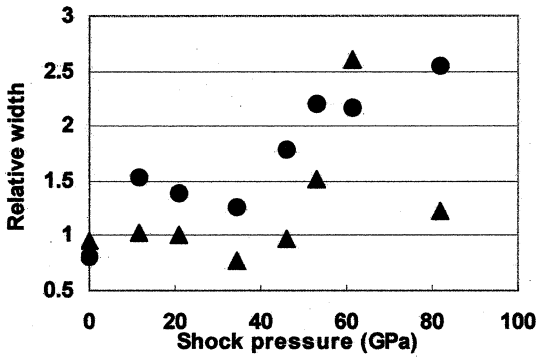

Figure4. Normalized Raman band width of Mg(M2)-O translational mode(307 cm^{-1}) vs the translational and rotational Si-O modes (230, 333 cm^{-1}) represented by triangles and circles, respectively.

while both translational vibrations of Mg-O and Si-O bands interfere with each other in more highly shocked forsterite.

Kudoh and Takeuchi (1985) have determined that the compressibilities of mean Si-O and Mg-O bonds of forsterite up to 14.9 GPa. At about 15 GPa, the Si-O bond was compressed by about 3.9 %, while the M2-O bond was about 3.6 % and that of the M1-O bond was 1.9 % relative to the value at ambient pressure. Contrasted to the variation of the M1-O bond which ceased at the compression 0.8 GPa, the Si-O and M2-O bonds were compressed linearly with increasing pressure. Kudoh et al. (1992) have developed ionic radius-bond strength systematics from these crystal structures. The linear compressibility coefficients of Si and Mg in olivine structure were 0.17 and 0.25, respectively.

Based on these data, Raman band shift and broadening of the Si-O bond with low compressibility, i.e. high bulk modulus K, which shows harder than Mg-O bond, are expected to be smaller than those of the Mg-O bond. Contrasted to the compressibility at static state, the variation of the band shift is only less than 1 % in the shocked forsterite (Fig. 2). The M2-O bond is only active in the Raman mode, therefore the present translational Mg-O vibration is due to the M2-O bond. The Si-O and M2-O bonds show similar pressure dependence under static state, however in shock state, as the tendencies above-mentioned or those shown in Figures 2 and 3, these two bonds are influenced differently by residual stress and strain in shock-experienced forsterite after shock-loading. Although the Si-O bond may be compressed as large as possible along with tetrahedral rotation, the M2-O bond may not compressed by preventing of the Si-O lattice and may be adapted to the strained Si-O lattice with

variable bond length. At shock event, M-O bond is softer than Si-O bond, therefore M-O bond must be strained and deformed extensively. These effects may reflect on the band shift as seen in Figures 2 and 3, and on the band width of the M2-O bond as follows.

In Figure 4, the variation of normalized band widths of the Mg-O band with the shock pressure are shown, where the widths are divided by the translational and rotational Si-O bandwidths of the same bands as in the cases of Figures 2 and 3. Scattering plots of the width and their larger attached error are visible. Especially, the normalized translational Mg-O bandwidth vs the rotational band of Si-O at near 333 cm^{-1} shows fewer scatters to the former, which is in accordance with the previous variation of their band shifts.

In Figure 5, the Mg-O bandwidth normalized by the internal asymmetric Si-O stretching band at around 548 cm^{-1} is shown to compare with that of Figure 4. The stretching Si-O band is not broadened as much as the Mg-O band with shifting to higher frequencies up to 46.2 GPa, while the Si-O band broadens irregularly at higher shock pressure more than 46.2 GPa, where the parameter of 548 cm^{-1} band can be obtained more precisely than the 333 cm^{-1} band. Although the Mg-O bandwidth itself is increased about three times to that of the non-shocked forsterite almost linearly with increasing pressure (Shinno et al., 2000a), the variation of the normalized widths is smoothed with the shock pressure below 40 GPa. Such relation is expressed:

$$W = 0.44(4) + 0.020(4) \times P - 0.00020(1) \times P^2 \quad (P < 40\text{GPa})$$

where W is normalized width with non-dimension, P shock pressure in GPa and the numbers in the parentheses are the standard deviations at the last decimal place.

These characteristic variations on Raman band parameters indicate that the deformation by the shock pressure takes place in a different manner in a crystal at the critical point of around 46.2 GPa. The positive stress within SiO_4 tetrahedra and negative stress in Mg(M2)-O octahedra less than 1 GPa still remain, judging from the pressure dependence of Raman band shifts shown in note under Table 1.

As the residual strain increases with shock pressure (Table 2), deformation in a shocked forsterite remains proportional with increasing loaded shock pressure less than 46.2 GPa. While above 46.2 GPa, the strain in the shocked forsterite may appear random judging from the irregularity of Raman band shifting and broadening.

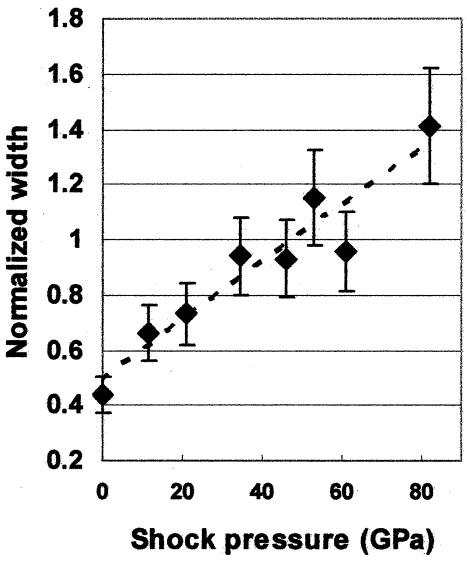

Figure 5. Normalized Raman band width of Mg(M2)-O translational mode(307 cm^{-1}) vs the internal Si-O asymmetric stretching (548 cm^{-1}) band.

In conclusion, the shock pressure of 46.2 GPa which nearly corresponds to the onset shock pressure of phase transition of 50 GPa on the Hugoniot curve of forsterite (Syono et al., 1981) and corresponds to the critical point of abrupt intensity change of the deformation sensitive luminescence (Shinno et al., 1999) is a meaningful critical point for the shocked forsterite. It is not clear that the point corresponds to those points of ceasing Mg(M1)-O bond shortening or at completion of the formation of oxygen hexagonal closest packing, as seen in Table 1. In any event, the critical shock pressure may show a higher-order of phase transition point on the shocked forsterites.

The pressure dependence of normalized width can be formulated, and the relation may be applied to estimate the shock pressure of chondritic olivines without chemical mass effect attached with their Raman bands.

Acknowledgment

I must pay my respects to the late Prof. S. Sueno, who had a broad view of things in mineralogy and stimulated my interest for new topics. I am deeply indebted to Dr. T. Nakamura of Kyushu University and to Dr. T. Sekine of the National Institute for Research in Inorganic Materials for providing study specimens. I also would like to express my thanks to reviewers for giving valuable and helpful comments.

References

Chopelas, A. (1990) Thermal properties of forsterite at mantle pressures derived from vibrational spectroscopy. Physics and Chemistry of Minerals, 17, 149-156.

Chopelas, A. (1991) Single crystal Raman spectra of forsterite, fayalite, and monticellite. American Mineralogist, 76, 1101-1109.

Heymann, D. (1990) Raman study of olivines in 37 heavily and moderately shocked ordinary chondrites. Geochimica et Cosmochimica Acta, 54, 2507-2510.

Heymann, D. and Cellucci, T. A. (1988) Raman spectra of shocked minerals 1: olivine. Meteoritics, 23, 353-357.

Hyde, B. G., White, T. J., O'Keeffe, M. and Johnson, A. W. (1982) Structures related to those of spinel and the β-phase, and a possible mechanism for the transformation olivine - spinel. Zeitschrift für Kristallographie, 160, 53-62.

Irifune, F., Nishiyama, N., Kuroda, K., Inoue, T., Isshiki, A., Utsumi, W., Funakoshi, K., Urakawa, T., Uchida, T., Katsura, T. and Ohtaka, O. (1998) Postspinel phase boundary in Mg_2SiO_4 determined by in situ X-ray diffraction. Science, 279, 1698-1670.

Jeanloz, R. (1980a) Shock effects in olivine and implications for Hugoniot data. Journal of Geophysical Research, 85, 3163-3176.

Jeanloz, R. (1980b) Infrared spectra of olivine polymorphs: α, β phase and spinel. Physics and Chemistry of Minerals, 5, 327-341.

Kudoh, Y. and Takeuchi, Y. (1985). The crystal structure of forsterite under high pressure up to 149 kb. Zeitschrift für Kristallographie, 171, 291-302.

Kudoh, Y., Prewwitt, C. T., Finger, L. W. and Ito, E. (1992). Ionic radius-bond strength systematics, ionic compressibilites, and an application to $(Mg,Fe)SiO_3$ perovskites. In High-Pressure Research: Application to Earth and Planetary Sciencies (Syono, Y. and Manghnani, M. H. Ed.), Terra Scientific Publisng Co. Tokyo. 215-218.

MacMillan, P. and Akaogi, M. (1987) Raman spectra of β-Mg_2SiO_4 (modified spinel) and γ- Mg_2SiO_4 (spinel). American Mineralogist, 72, 361-364.

McMillan, P., Wolf, G. and Lambert, P. (1992) A Raman spectroscopic study of shocked single crystalline quartz. Physics and Chemistry of Minerals, 19, 71-79.

Madon, M. and Poirier, J. P. (1983) Transmission electron microscope observation of α, β and γ-$(Mg,Fe)_2SiO_4$ in shocked meteorites: planar defects and polymorphic transitions. Physics of Earth Planetary Interiors, 33, 31-44.Miyamoto, M. and Ohsumi, K. (1995). Micro Raman spectroscopy of olivines in L6 chondrites: Evaluation of the degree of shock. Geophysical Research Letters, 22, 437-440.

Morishima, H., Kato, T., Suto, M., Ohtani, E., Urakawa, S., Utsumi, W., Shimonura, O. and Kikegawa, T. (1994) The phase boundary between α- and β-Mg_2SiO_4 determined by in situ X-ray observation. Science, 265, 1202-1203.

Ooba, T. and Shinno, I. (1996) Evaluation of shocked pressure in olivine of the Antarctic meteorites YAMATO 790523 and 790575. Abstract, Annual Meeting of Japanese Mineralogical Society, 62 (in Japanese).

Paques-Ledent, T. TH. and Tarte, P. (1973) Vibrational studies of olivine-type compounds - I. The I.R. and Raman spectra of the isotopic species of Mg_2SiO_4. Spectrochimica Acta, 29A, 1007-1016.

Price, G. D., Parker, S. C. and Leslie, M. (1987) The lattice dynamics of forsterite. Mineralogical Magagine, 51, 157-170.

Reynard, B., Petit, P., Guyot, F. and Gillet, P. (1994) Pressure-induced structural modifications in Mg_2GeO_4-olivine: A Raman spectroscopic study. Physics and Chemistry of Minerals, 20, 556-562.

Reynard, B., Takir, F., Guyot, F., Gawanmesia, G. D., Liebermann, R. C. and Gillet, P. (1996) High-temperature Raman spectroscopic and X-ray diffraction study of β-Mg_2SiO_4 : Insights into its high-temperature thermodynamic properties and the β- to α-phase-transformation mechanism and kinetics. American Mineralogist, 81, 585-594.

Servoin, J. L. and Piriou, B. (1973) Infrared reflectivity and Raman scattering of Mg_2SiO_4 single crystal. Physics and Chemistry of Minerals, 55, 677-686.

Shinno, I., Nakamuta, Y., Nakamura, T. and Sekine, T. (1999) Characterization of artificially shocked forsterites: (2) Profile analysis of photo-luminescence spectra. Mineralogical Journal, 21, 119-130.

Shinno, I., Nakamuta, Y., Nakamura, T. and Sekine, T. (2000a) Characterization of Artificially Shocked Forsterites: (3) Profile analysis of Raman spectra. Mineralogical Journal, 22, 11-20.

Shinno, I., Nakamura, T. and Sekine, T. (2000b) Deformation-sensitive luminescence of forsterite (Mg_2SiO_4) shocked up to 82 GPa. Journal of Luminescence, 87-89, 1292-1294.

Suzuki, A., Ohtani E., Morishima, H., Kubo, T., Kanbe, Y., Kondo, T., Okada, T., Terasaki, H., Kato, T. and Kikegawa, T. (2000) In situ determination of the phase boundary between wadsleyite and ringwoodite in Mg_2SiO_4. Geophysical Research Letters, 27, 803-806.

Syono, Y., Goto, T., Sato, J. and Takei, H. (1981) Shock compression measurements of single-crystal forsterite in the pressure range 15-93 GPa. Journal of Geophysical Research, 86, B7, 6181-6186.

Uchizono, A., Shinno, I., Nakamuta, Y., Nakamura, T and Sekine, T. (1999) Characterization of artificially shocked forsterites: (1) Diffraction profile analysis by Gandolfi Camera. Mineralogical Journal, 21, 15-23.

Wang, S. Y., Sharma, S. K. and Cooney, T. F. (1993) Micro-Raman and infrared spectral study of forsterite under high pressure. American Mineralogist, 78, 469-476.

Wilson, A. J. C. (1962) X-ray Optics. 1-5, John Wiley & Sons, New York.

Manuscript received; 22 February, 2002
Manuscript accepted; 31 May, 2002